

Pressure-induced structural transformations in glass $0.3\text{Li}_2\text{O}-0.7\text{B}_2\text{O}_3$: A molecular dynamics study

A. Vegiri* and E. I. Kamitsos

*Theoretical and Physical Chemistry Institute, National Hellenic Research Foundation, 48 Vassileos Constantinou Avenue,
116 35 Athens, Greece*

(Received 28 April 2010; revised manuscript received 24 June 2010; published 20 August 2010)

Molecular dynamics (MD) simulations were used to study structural transformations in glass $0.3\text{Li}_2\text{O}-0.7\text{B}_2\text{O}_3$ induced by high pressure up to 300 GPa. Pressure-induced coordination changes were found to involve the gradual transformations of boron $^{[3]}\text{B} \rightarrow ^{[4]}\text{B} \rightarrow ^{[5]}\text{B} \rightarrow ^{[6]}\text{B}$ and the transformations $^{[2]}\text{O} \rightarrow ^{[3]}\text{O} \rightarrow ^{[4]}\text{O}$ of oxygen, where superscripts in brackets indicate coordination numbers. Four different pressure zones were distinguished by probing the relative population of boron and oxygen atoms in different coordination states, and found to correspond to pressures below 5 GPa (I), 5–15 GPa (II), 15–80 GPa (III), and 80–300 GPa (IV). The results of MD simulations are in good agreement with reported findings by inelastic x-ray scattering for pressures up to 30 GPa attainable currently by experiment. More detailed structural information was obtained by MD for zone III where the boron and oxygen coordination numbers were found constant at $\text{B}[\text{O}]=4$ and $\text{O}[\text{B}]\approx 2.35$ in a broad pressure range. It was shown that the structure of glass in this zone is consistent with the engagement of 91.5% of four-coordinated boron atoms, $^{[4]}\text{B}$, in tricluster arrangements where three $^{[4]}\text{B}$ atoms are corner sharing the same three-coordinated oxygen atom, $^{[3]}\text{O}$, and have the overall stoichiometry of $[\text{B}_3\text{O}_2]^{-1}$. While this tricluster is the dominant structural element, the remaining 8.5% of $^{[4]}\text{B}$ atoms are found in tetrahedral borate units which involve nonbridging oxygen atoms (approximately 4.3%) as well as $^{[3]}\text{O}$ and $^{[2]}\text{O}$ oxygen atoms.

DOI: [10.1103/PhysRevB.82.054114](https://doi.org/10.1103/PhysRevB.82.054114)

PACS number(s): 61.43.Bn, 62.50.-p, 61.43.Fs

I. INTRODUCTION

Vitreous boron oxide, $v\text{-B}_2\text{O}_3$, together with $v\text{-SiO}_2$ and $v\text{-GeO}_2$ constitute prototypical glass-forming systems. Because of their technological importance these glasses have received broad attention both experimentally and theoretically, either in their pure state or when doped with metal oxides to give more complex glasses. However, the great majority of experiments have been conducted at atmospheric pressure or on pressure-released glasses due to difficulties in extending the available diffraction techniques to elevated pressures, a problem arising mainly from the poor signal-to-noise ratio at high pressures.¹ *In situ* Raman, neutron, and Brillouin scattering, as well as synchrotron x-ray techniques applied to low atomic number oxide glasses, such as borates, yield unambiguous results only at relatively low pressures below about 10 GPa.^{2,3}

High-pressure studies are of particular interest to geologists in their attempt to understand structural, thermodynamic, and transport properties of magma in the earth's interior. In this context, structural studies at the microscopic level would prove valuable. Compared to silicates, which have received the lion's share in the corresponding literature,^{1,4-12} little is known about the behavior of borates under the same conditions. In particular, while the majority of related experimental¹³⁻¹⁸ and theoretical¹⁹⁻²¹ studies deal with structural transformations of *ex situ*^{13,14} and *in situ*¹⁵⁻¹⁸ compressed B_2O_3 there are only two reports on experimental investigation of the structure of compressed binary borate glasses.^{2,3} The *in situ* experimental study of coordination number changes in $v\text{-B}_2\text{O}_3$ (Ref. 18) at pressures up to 30 GPa, as well as in Li-diborate² and Na-diborate³ glasses, became possible due to application of the so-called synchrotron inelastic x-ray scattering technique.

In the following, we present briefly similarities and differences in the densification mechanism of the three archetypal glasses mentioned above. The chemically and structurally equivalent $v\text{-SiO}_2$ and $v\text{-GeO}_2$ consist at atmospheric pressure of a continuous random network of SiO_4 and GeO_4 tetrahedra which are linked by corner-shared oxygen atoms. As a consequence, silica and germania glasses share several properties. When pressure is applied above a certain threshold the network-forming Si and Ge ions experience a gradual coordination change from fourfold to fivefold and to sixfold, with the notion that fivefold-coordinated oxygen atoms have not been observed experimentally, but this conversion is not retained in the decompressed glass which returns eventually to its original fourfold coordination.^{4-7,9,11,22-26} Nevertheless, after a compression-decompression cycle the glass is found in a permanently densified state, up to 20% in silica and to a maximum of $\sim 17\%$ in germania,²⁷ provided that the pressure from where the glass is decompressed is above a certain threshold value. The threshold pressure for permanent densification amounts to $\sim 10\text{--}12$ GPa for silica^{6,11} and to ~ 5 GPa for germania,^{22,23} indicating an increased sensitivity of the latter glass to pressure.

In contrast to silica and germania, $v\text{-B}_2\text{O}_3$ at ambient temperature and pressure consists of a random network of planar triangular BO_3 units and boroxol rings, the fraction of which is still a matter of debate, see Refs. 21 and 28. Although from the structural point of view borates belong to a different family of glasses, their overall response to pressure is not very different from that of silicates and germanates. For example, upon compression above a threshold value of ~ 5 GPa and subsequent decompression borate glasses show residual densification,^{16,19} with a densification ratio varying from 6% to 11% depending on the conditions of treatment²⁰ according

to result from simulations. The densified glass is characterized by the breakup of boroxol rings and the buckling of “ribbons” formed by BO_3 triangles.¹⁹ However, no changes in the boron coordination sphere and in the short-range order structure have been observed in densified $v\text{-B}_2\text{O}_3$. Above the threshold pressure of ~ 5 GPa threefold-coordinated boron atoms transform gradually into fourfold ones,^{2,3,18} and the characteristic boroxol rings are destructed completely at pressures greater than ~ 14 GPa, as shown in *ex situ*¹⁴ and *in situ*¹⁵ experiments and in simulations.¹⁹ Simulations show also that at pressures exceeding 150 GPa polyhedra BO_5 and BO_6 start to form in increasing proportions.¹⁹

The threefold to fourfold transformation of boron atoms can be induced also by chemical routes besides pressure. This includes the addition of network-modifying metal oxides to vitreous B_2O_3 even at ambient pressure. For example, the mole fraction of fourfold-coordinated boron atoms in lithium-borate glasses $x\text{Li}_2\text{O}-(1-x)\text{B}_2\text{O}_3$ would be $x/(1-x)$ if creation of fourfold-coordinated boron atoms is the only structure transformation mechanism (x is the mole fraction of Li_2O). However, addition of modifier metal oxides to B_2O_3 could lead also to formation of nonbridging oxygen atoms (NBOs) through breaking of B-O-B linkages. At ambient conditions, NBOs are bonded to triangular borate units and contribute to the depolymerization of the borate network. The degree of threefold to fourfold transformation of B atoms and, thus, the amount of NBO formation depend highly on the type and molar fraction of the modifier metal oxide.²⁹ In this context, it is of interest to study the compression behavior of a binary borate glass which, in contrast to $v\text{-B}_2\text{O}_3$, involves already a proportion of fourfold-coordinated boron atoms.

Recently, Lee *et al.*² performed *in situ* synchrotron inelastic x-ray scattering studies on Li-diborate glass, $0.33\text{Li}_2\text{O}-0.67\text{B}_2\text{O}_3$, with pressure spanning the range from ambient to 30 GPa. This experiment revealed three distinct zones corresponding to different densification mechanisms. For pressures less than about 5 GPa the decrease in the fraction of threefold-coordinated boron atoms, $^{[3]}\text{B}$, was small (approximately 15%) whereas $^{[3]}\text{B}$ was found to decrease rapidly in the region 5–12 GPa. For pressures exceeding 15 GPa the rate of structural transformation was significantly reduced as almost all boron atoms had acquired the fourfold coordination. In a similar study of Na-diborate glass Lee *et al.*³ found that $^{[3]}\text{B}$ decreases almost linearly for pressures up to 25 GPa, a behavior that contrasts the nonlinear transformation exhibited by Li-diborate glass.² Thus, it was suggested that the different transformation behaviors of Li- and Na-diborate glasses arise from differences in cation field strength and that the nature of the charge-balancing cation affects the stability of the borate topology at high pressure.³

We have studied by molecular dynamics (MD) at ambient pressure the structure of alkali borate glasses of composition $0.3[(1-x)\text{Li}_2\text{O}-xM_2\text{O}]-0.7\text{B}_2\text{O}_3$, $M=\text{Na}, \text{Cs}$, and $0 \leq x \leq 1$, and were able to reveal the effect of the charge-balancing alkali cations on the local borate structure of both single and mixed alkali glasses.^{30,31} The present work presents a molecular dynamics study of the binary glass $0.3\text{Li}_2\text{O}-0.7\text{B}_2\text{O}_3$ from ambient to 300 GPa, this range of pressures exceeding greatly those accessible currently by

experiment.^{2,3} The purpose of this work is to investigate at the microscopic level the densification mechanism of Li-borate glasses and to contribute toward a better understanding of pressure-induced transformation phenomena in the poorly investigated binary borate glasses.

II. COMPUTATIONAL DETAILS

As in our previous molecular dynamics studies of single³⁰ and mixed alkali borate glasses,³¹ we employed here a Born-Mayer-Huggins type of potential with three-body harmonic interactions for the O-B-O angles, which was fitted to experimental radial distribution functions and to infrared and Raman spectra at ambient conditions.³² Molecular dynamics simulations were carried out with the help of the DLPOLY program³³ at the NVT ensemble at $T=300$ K. Integration time was set to 1 fs and the relaxation time in the Berendsen thermostat was 0.01 ps for the stabilization of temperature at high pressures.

We used an ensemble of 1020 particles, from which 556 were oxygen atoms, 324 boron atoms, and 140 Li ions. The initial box size was set at $L=21.494$ Å corresponding to the experimental density of 2.235 g/cm³,³⁴ whereas the initial configuration was taken after heating the system at 5000 K and then letting it cool in five consecutive cycles until room temperature was reached. At each cycle the system was equilibrated for a few picoseconds, except at the last cycle where aging was for a much longer time of 3 ns. Properties were gathered for the next nanosecond. The last configuration of each run served as the starting configuration for the next run at a higher density, corresponding to a higher pressure. Again, aging was for 3 ns and properties were collected for the next 1 ns. In total, we performed 12 different calculations for pressures up to about 300 GPa namely, at $P=3.9, 4.7, 7.24, 10.15, 15.8, 24.7, 34.9, 56.5, 81.4, 119.5, 168.3, \text{ and } 318.7$ GPa, which correspond to densities 2.235, 2.298, 2.433, 2.578, 2.772, 2.991, 3.183, 3.503, 3.803, 4.13, 4.514, and 5.414 g/cm³.

It is noted that the glass resulting from the model potential at the experimental density is not at atmospheric pressure. This is a known artifact in several model potentials, leading to calculated density deviating from the experimental one. Thus, when the structure of the studied glass $0.3\text{Li}_2\text{O}-0.7\text{B}_2\text{O}_3$ is that of the glass under atmospheric pressure the calculated pressure is 3.9 GPa instead of ambient. To account for this effect we have shifted the calculated pressure values by 3.9 GPa. Thereafter we denote the shifted pressure by P .

III. RESULTS AND DISCUSSION

A. Short- and medium-range order structures

The relative population of three-coordinated boron atoms, $^{[3]}\text{B}$, has been calculated as usually^{30,31} from the corresponding B-O radial distribution functions (RDFs). The results are shown in Fig. 1 as a function of the shifted pressure P and they are also compared with the experimental data reported for Li-diborate glass.² Taking into account the experimental error in Fig. 2 of Ref. 2, we suggest that the present MD

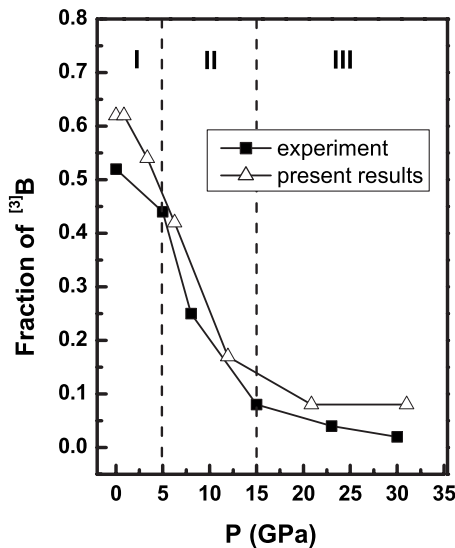


FIG. 1. Effect of pressure on the fraction of three-coordinated boron atoms, $^{[3]}B$, as obtained by MD simulations for glass $0.3Li_2O-0.7B_2O_3$ (triangles) and by inelastic x-ray scattering (Ref. 2) for Li-diborate glass (squares). Dashed lines are guides to the eye to mark different pressures zones (I, II, and III).

results are in very good agreement with experiment. The systematic upward shift of the calculated curve with respect to experiment can be well justified in terms of the Li_2O mole fraction which is $x=0.30$ for the present study and $x=0.33$ for the experimental investigation.² Thus, the theoretical fraction of threefold-coordinated boron atoms at atmospheric pressure, $^{[3]}B=1-(x/1-x)$, would be 0.57 for the present study and 0.51 for the experimental glass, which is well consistent with the trend observed in Fig. 1.

The calculated $^{[3]}B$ fraction displays a pressure dependence which is nearly the same as that observed in experiment (Fig. 1); it shows a small reduction at pressures below 5 GPa (zone I), a fast decrease in the 5–15 GPa range (zone II), and a slow variation for higher pressures (zone III). We note that the computed zone I was rather limited compared to experiment and restricted to pressures P below 1 GPa. Also, none of the variations in $^{[3]}B$ was found to be so abrupt as to signify the onset of a first-order-like structural transition as it occurs, for example, in crystals.

Besides the *in situ* inelastic x-ray scattering results² and the present MD simulations, fluorescence lifetime measurements at room temperature and high pressures on Eu^{3+} -doped $0.67Li_2O-0.33B_2O_3$ glass show also the existence of three distinct pressure zones up to 30 GPa.³⁵ Namely, the fluorescence lifetime changes only marginally up to ~ 5 GPa, then it decreases rapidly from ~ 5 to ~ 15 GPa and from ~ 15 GPa and beyond it varies very slowly. This result was attributed to pressure-induced structural changes in the borate network.³⁵

In the following, we analyze in detail the underlying structural transformations not only in the experimental pressure range but also at much higher pressures investigated by MD, i.e., from ~ 30 to ~ 300 GPa. Our calculations show that the pressure regime above 80 GPa, denoted thereafter as zone IV, marks the onset of new kind of structural transformations.

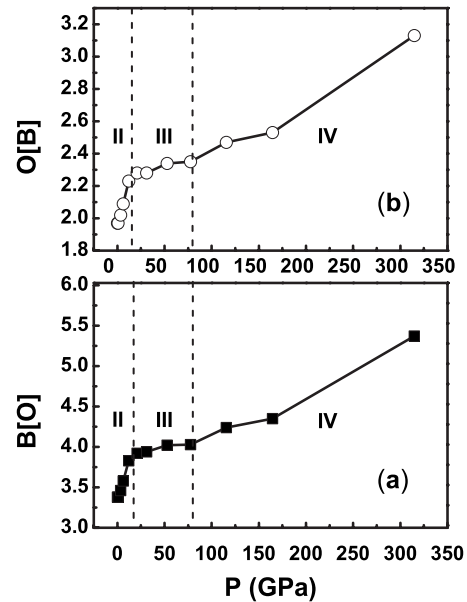


FIG. 2. Pressure dependence of the boron, $B[O]$, and oxygen, $O[B]$, coordination numbers for glass $0.3Li_2O-0.7B_2O_3$. Dashed lines are guides to the eye to mark different pressures zones.

The $B[O]$ and $O[B]$ coordination numbers are displayed in Fig. 2 where, apart from zone I which is very narrow, zones II, III, and IV are easily distinguishable. Zone II manifests the $^{[3]}B$ to $^{[4]}B$ transformation of B atoms and displays the largest gradient for both $B[O]$ and $O[B]$ coordination numbers. It is well known that boron coordinates with oxygen to form stable triangular and tetrahedral borate units, the latter having smaller effective volume than the triangular borate unit.³⁶ The same effect was observed in simulations of compressed silicates and germanates where pressure induces the transformation of fourfold Si and Ge atoms to fivefold and sixfold ones.

Figure 2 shows that zone III does not die out at 30 GPa, which was the highest pressure attainable by experiment, but it extends to approximately 80 GPa. The $B[O]$ coordination number remains constant at $B[O] \approx 4$ in a broad plateau region from ~ 15 to ~ 80 GPa [Fig. 2(a)], indicating the absence of major structural transformations. The same applies to $O[B]$ in zone III which varies from 2.28 to 2.35, implying a borate structure with approximately one third of its oxygen atoms being coordinated to three boron tetrahedral units. Triply bonded oxygen to three tetrahedral units, known as tricluster oxygen ($^{[3]}O$), was first observed in the high-pressure form of crystalline boron oxide, B_2O_3 II,³⁷ and more recently in B_2O_3 glass and crystal at high pressures.^{13,19-21} Inspection of Fig. 2 shows that tricluster-type structural arrangements should appear also in zone II of glass $0.3Li_2O-0.7B_2O_3$ although to a lesser extent than in zone III.

For pressures above approximately 80 GPa (zone IV) the slope of the curves in Fig. 2 start rising again manifesting the formation of structures which, for energetic reasons, are not stable at lower pressures. Thus, Fig. 2(a) shows that boron atoms with fivefold and sixfold coordination are created in zone IV with their population increasing with pressure. For instance, our calculation shows that five-coordinated B at

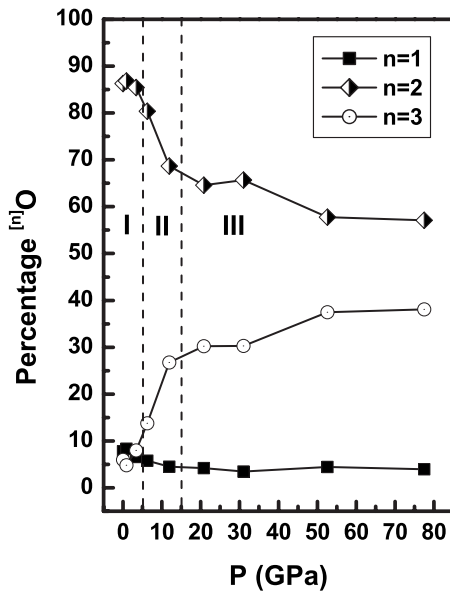


FIG. 3. Pressure dependence of the relative population of oxygen atoms in the three coordination states; nonbridging ($^{[1]}\text{O}$), twofold coordination ($^{[2]}\text{O}$), and threefold coordination ($^{[3]}\text{O}$) for glass $0.3\text{Li}_2\text{O}-0.7\text{B}_2\text{O}_3$.

oms represent 6% of all B atoms at 77.5 GPa, this value increasing to 26% at 164.4 GPa and to 45% at 315 GPa. Similarly, six-coordinated boron represents 3% of the total B population at 164.4 GPa and almost 50% at 315 GPa. Also, the population of threefold-coordinated O atoms in zone IV increases steadily at the expense of two-coordinated O atoms [Fig. 2(b)]. In the following, we will extend further our structural analysis for glasses pressurized in zones II and III.

At atmospheric pressure oxygen is present in glass $0.3\text{Li}_2\text{O}-0.7\text{B}_2\text{O}_3$ mainly in twofold coordination, $^{[2]}\text{O}$, with a small proportion (approximately 8% in this work) of O atoms being NBOs, $^{[1]}\text{O}$, i.e., bonded to one B atom in borate triangles. The population of O atoms in the three coordination states, $^{[1]}\text{O}$, $^{[2]}\text{O}$, and $^{[3]}\text{O}$, is shown in Fig. 3 as a function of pressure. Oxygen in fourfold coordination, $^{[4]}\text{O}$, was found in small amounts only in zone IV, and it requires pressures as high as 300 GPa to reach a significant fraction (27%). For pressures lower than 80 GPa the $^{[2]}\text{O}$ and $^{[3]}\text{O}$ fractions evolve in a complementary fashion while the NBO fraction tends to decrease with increasing pressure (Fig. 3). NBOs in zone III are located on boron tetrahedral units and represent about 4% of the entire oxygen population, this fraction reducing to 2% at $P=315$ GPa. For this reason, we suggest that the role of NBOs in glass restructuring in zones III and IV is negligible. In zone II NBOs are consumed for the transformation of threefold B atoms to fourfold ones.

A key feature of Fig. 3 is that at the high-pressure side of zone III the ratio of oxygen populations in bonding states $^{[2]}\text{O}$ and $^{[3]}\text{O}$ is found to be $^{[2]}\text{O}/^{[3]}\text{O}=1.5$, i.e., for every three $^{[2]}\text{O}$ atoms there are two $^{[3]}\text{O}$ atoms. We will explore further this important finding in Sec. III C.

The $^{[2]}\text{O}$ and $^{[3]}\text{O}$ populations can be examined in more details according to the structural configuration of the neighboring boron atoms. For example, an $^{[2]}\text{O}$ atom can be coor-

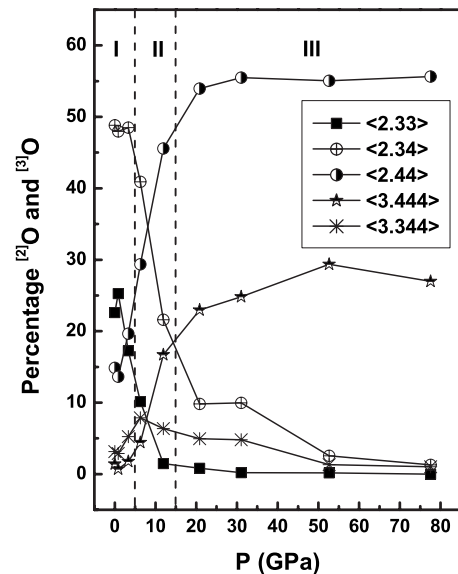


FIG. 4. Pressure dependence of the relative population of $^{[2]}\text{O}$ and $^{[3]}\text{O}$ oxygen atoms bonded to $^{[3]}\text{B}$ and/or $^{[4]}\text{B}$ boron atoms for glass $0.3\text{Li}_2\text{O}-0.7\text{B}_2\text{O}_3$. The first number in the notation (see inset) gives the coordination state of O and the following two or three numbers give the coordination of the first neighbor B atoms.

ordinated to two borate triangles, to two tetrahedra, or to one triangle and one tetrahedron. A similar situation applies to $^{[3]}\text{O}$ atoms for which the possible bonding combinations are four. The percentage populations of the resultant configurations are shown in Fig. 4, where the first number in the notation gives the coordination state of the O atom under consideration and the following two or three numbers give the coordination state of the first neighbor B atoms. For instance, notation $\langle 3.344 \rangle$ refers to a threefold-coordinated O atom which is bonded to one three-coordinated and to two four-coordinated B atoms.

As shown in Fig. 4 the most abundant configuration at atmospheric pressure is the $\langle 2.34 \rangle$ one because of the almost equal populations of triangular and tetrahedral borate units (Fig. 1). The next important configuration is the $\langle 2.33 \rangle$ followed by $\langle 2.44 \rangle$. This ordering changes rapidly in zone II and the dominant configurations in the plateau region (zone III) are the $\langle 2.44 \rangle$ and $\langle 3.444 \rangle$ ones. This result is consistent with the almost complete disappearance of three-coordinated boron atoms in zone III [Fig. 2(a)]. Thus, the remaining $\langle 2.34 \rangle$ and $\langle 3.344 \rangle$ configurations represent only 2–4% of the total O population in the high-pressure end of zone III.

Up to this point we have considered the response of glass to pressure by examining the transformation of short-range order structural units and their interconnectivity. We focus now on bond angle and bond length variations in zones II and III starting with the effect of pressure on the $\text{O}-^{[3]}\text{B}-\text{O}$ and $\text{O}-^{[4]}\text{B}-\text{O}$ angle distributions (Fig. 5). The $\text{O}-^{[3]}\text{B}-\text{O}$ distribution in Fig. 5(a) shows that the borate triangles remain intact in zone II, whereas they experience a significant angular contraction by approximately 5° in zone III leading to distortion of their planarity. We recall that the $^{[3]}\text{B}$ population in zone III is very small (Fig. 1) due to the almost complete transformation of triangular units into borate tetrahedral. Re-

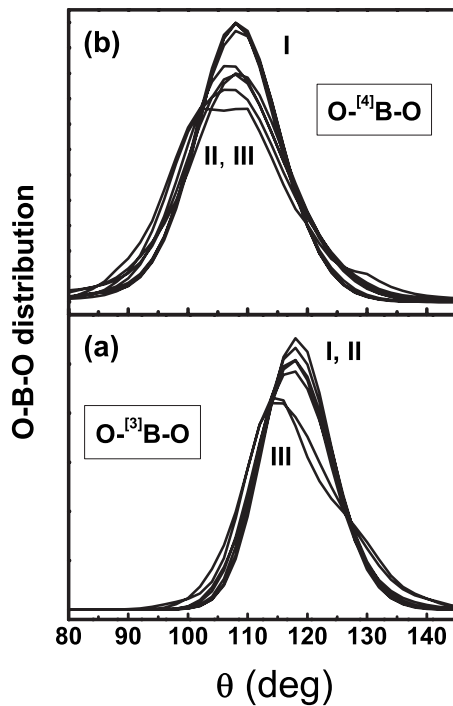


FIG. 5. Effect of pressure on the $O-[^3]B-O$ and $O-[^4]B-O$ angle distributions for glass $0.3Li_2O-0.7B_2O_3$. Pressures from top to bottom in frame (a) are 0, 0.85, 3.4, 6.8, 12, 20.9, and 31 and in frame (b) 0, 0.85, 3.4, 6.8, 12, 20.9, 31, 52.6, and 77.5 GPa.

garding the $O-[^4]B-O$ distribution, Fig. 5(b) shows that pressure causes a progressive but insignificant contraction of the tetrahedral angles except at the edge of zone III, where the departure from a regular tetrahedron is about 2° . In addition, the $O-[^4]B-O$ distribution in zone III broadens considerably relative to that in zone II. Nevertheless, the angles of the borate tetrahedral units remain rather uncompressed despite the considerable pressure applied to glass in zone III and they continue to remain so even at higher pressures in zone IV (not shown here).

Compared to O-B-O the B-O-B angle distribution is much more sensitive to pressure as observed in Fig. 6. At atmospheric pressure the B-O-B distribution peaks at 145° , whereas as a larger population of oxygen atoms becomes threefold coordinated with pressure increase, the B-O-B distribution shifts and centers around 120° , in accordance with the appearance of structural arrangements around tricluster $[^3]O$ atoms. However, the B-O-B distribution remains considerably broader compared to $O-[^4]B-O$. Therefore, tricluster formation and broad angular distributions present aspects of the glass response to increasing pressure in zone III.

The calculated radial distribution functions for B-O bond lengths in triangular, $[^3]B-O$, and tetrahedral units, $[^4]B-O$, are presented Fig. 7 and verify the expected bond contraction with pressure. However, bond lengths start to be affected only for pressures at the onset of zone III. At lower pressures, the transformation of triangular to tetrahedral units takes place without any significant geometrical distortion either in angles (Fig. 5) or in bond lengths (Fig. 7). For pressures up to 77.5 GPa the B-O length contraction in tetrahedral units is about 0.05 \AA , i.e., from 1.429 to 1.377 \AA while

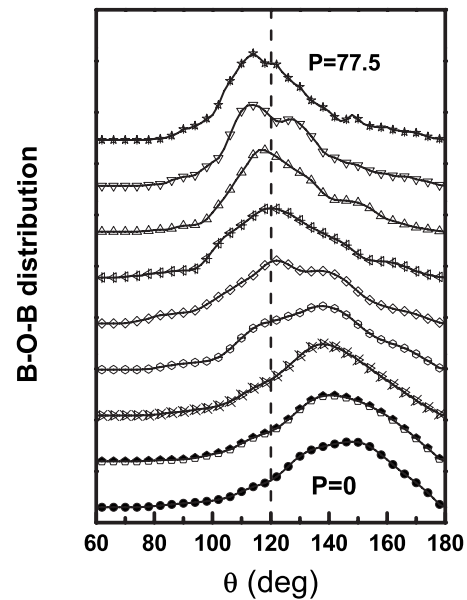


FIG. 6. Effect of pressure on the B-O-B angle distribution for glass $0.3Li_2O-0.7B_2O_3$. Pressures from bottomup are at 0, 0.85, 3.4, 6.8, 12, 20.9, 31, 52.6, and 77.5 GPa.

B-O decreases to a smaller extent in borate triangles (about 0.025 \AA , from 1.340 \AA to 1.315 \AA).

While Fig. 7(b) presents the effect of pressure on the overall $[^4]B-O$ bonding one can now distinguish between $[^4]B-[^2]O$ and $[^4]B-[^3]O$ bonds where fourfold B atoms are bonded to twofold and threefold O atoms, respectively. Figure 8 shows that pressure has opposite effects on the $[^4]B-[^2]O$ and $[^4]B-[^3]O$ bonds; the first contracting [Fig. 8(a)] and the second expanding [Fig. 8(b)] at higher pressures.

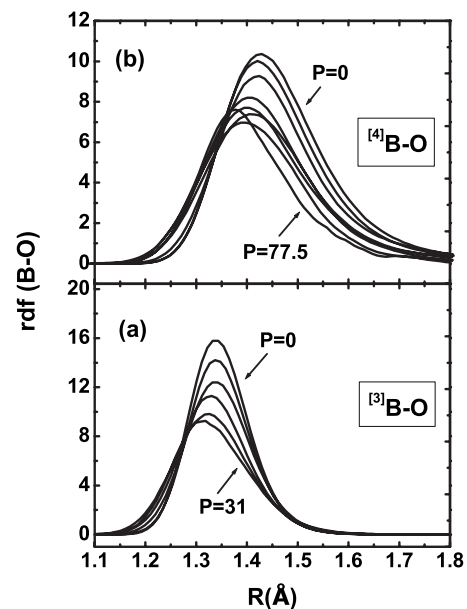


FIG. 7. Radial distribution functions for B-O bonds in triangular ($[^3]B-O$) and tetrahedral ($[^4]B-O$) borate units as a function of pressure for glass $0.3Li_2O-0.7B_2O_3$. Pressures from top to bottom are in frame (a) at 0, 3.4, 6.8, 12, 20.9, and 31 GPa, and in frame (b) at 0, 3.4, 6.8, 12, 20.9, 31, 52.6, and 77.5 GPa.

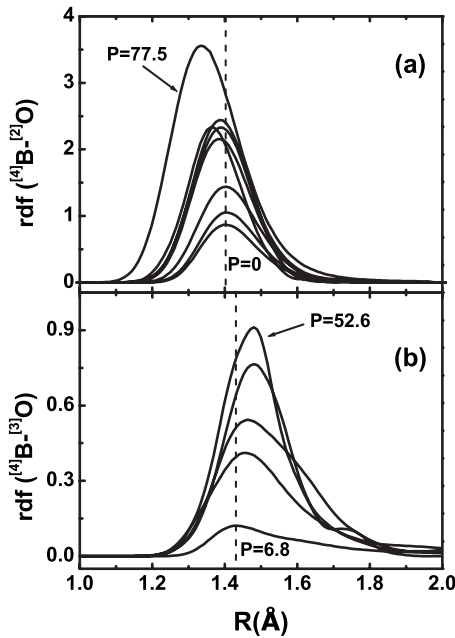


FIG. 8. Radial distribution functions for $[4]B-[2]O$ and $[4]B-[3]O$ bonds as a function of pressure for glass $0.3Li_2O-0.7B_2O_3$. Pressures from bottomup are in frame (a) at 0, 3.4, 6.8, 12, 20.9, 31, 52.6, and 77.5 GPa, and in frame (b) at 6.8, 12, 20.9, 31, and 52.6 GPa.

This finding for Li-borate glass is in agreement with observations made on borate systems having tricluster configurations in their structure. For example, in the high-pressure form of crystalline boron oxide (B_2O_3 II) the borate tetrahedral units are highly distorted with three long B-O distances of 1.506, 1.507, and 1.512 Å and a shorter B-O distance of 1.373 Å.³⁷ The oxygen atoms associated with the former distances are coordinated by three boron atoms, $[3]O$, whereas the oxygen in the short B-O bond is twofold coordinated by boron atoms, $[2]O$.

B. Li-ion environments

Rather than presenting an overall Li-O RDF, we prefer to calculate separate radial distribution functions for Li cations coordinated to $[2]O$ and $[3]O$ oxygen atoms. The corresponding RDFs are shown in Fig. 9 for four different pressures, two of which correspond to zone II [Figs. 9(a) and 9(b)] and two to zone III [Figs. 9(c) and 9(d)]. Irrespective of the applied pressure, two distinctly different behaviors are observed depending on whether Li cations are coordinated to $[2]O$ or to $[3]O$ oxygen atoms. In the first case the Li ions occupy well-defined sites, as inferred from the sharp and well structured first shell in the corresponding RDF, whereas when Li is close to $[3]O$ in a tricluster unit the first shell structure is almost completely destroyed. This effect could be related to the greater delocalization of charge around the $[3]O$ tricluster oxygen, leading to weaker electrostatic interactions between Li cations and $[3]O$ oxygen atoms.

C. Tricluster structures in Li-borate glass under high pressure

As presented above, the short-range order structure of glass $0.3Li_2O-0.7B_2O_3$ in the high-pressure side of zone III

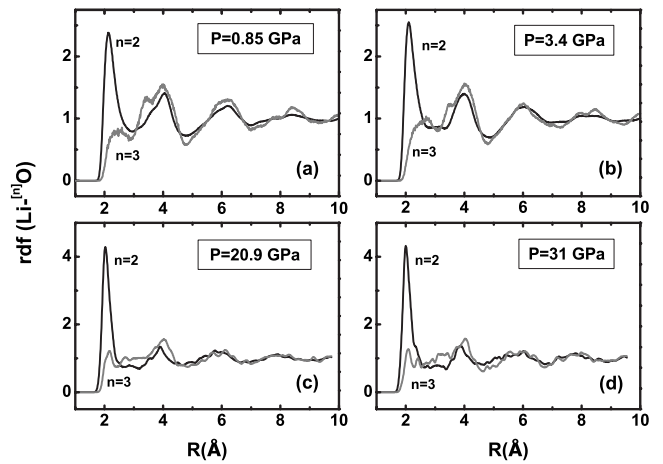


FIG. 9. Effect of pressure on the Li-O radial distribution functions for Li ions coordinated to $[2]O$ ($n=2$) and $[3]O$ ($n=3$) oxygen atoms for glass $0.3Li_2O-0.7B_2O_3$.

is characterized by $B[O]=4$ and $O[B]=2.35$ (Fig. 2). The average oxygen coordination value of 2.35 arises from the fact that oxygen is present in the three coordination states shown in Fig. 3; threefold, $[3]O$, twofold, $[2]O$, and NBO, $[1]O$. Therefore, the key element of this borate structure should be tricluster-type arrangements where three tetrahedral boron atoms, $[4]B$, are bonded to the same oxygen atom, $[3]O$. Such triclusters should constitute the major part of glass structure and coexist with minor structural elements where NBOs are bonded to $[4]B$ atoms. The overall glass structure in the high-pressure end of zone III should be consistent with the MD findings in Figs. 2 and 3, $O[B]=2.35$, $[2]O/[3]O = 1.5$, and $[1]O \approx 4.3\%$, and it should respect the composition of the simulated glass, i.e., $0.3Li_2O-0.7B_2O_3$.

The presence of tricluster arrangements at high pressures has been suggested for Li-diborate and Na-diborate glasses by the inelastic x-ray scattering studies of Lee *et al.*^{2,3} These studies have focused on the pressure-induced coordination transformation of boron but no structure was suggested for the triclusters formed at high pressures. In this context, it is challenging to employ here the MD results and explore the tricluster structures formed in glass $0.3Li_2O-0.7B_2O_3$ at the end of zone III.

As a guide to our approach we consider first the high-pressure form of crystalline boron oxide (B_2O_3 II) formed by quenching powdered B_2O_3 from 6.5 GPa and 1200 °C.³⁷ The structure of B_2O_3 II was found to consist of corner-linked BO_4 tetrahedra having three $B-[3]O$ bonds and one $B-[2]O$ bond, where in the overall structure two thirds of oxygen atoms are $[3]O$ and one third $[2]O$.³⁷ Three borate tetrahedra bonded to the same $[3]O$ oxygen give the tricluster arrangement of B_2O_3 II shown schematically in Fig. 10(a). It can be easily verified that this tricluster corresponds to neutral B_2O_3 as it should.

Tricluster arrangements have been found also in metal-borate crystals where they increase the borate network connectivity and serve as charge compensation and compression mechanisms. Examples are the $PbO \cdot 2B_2O_3$ crystal prepared at atmospheric pressure,³⁸ and the $\beta-ZnB_4O_7$ crystal synthesized under high-pressure and high-temperature conditions.³⁹

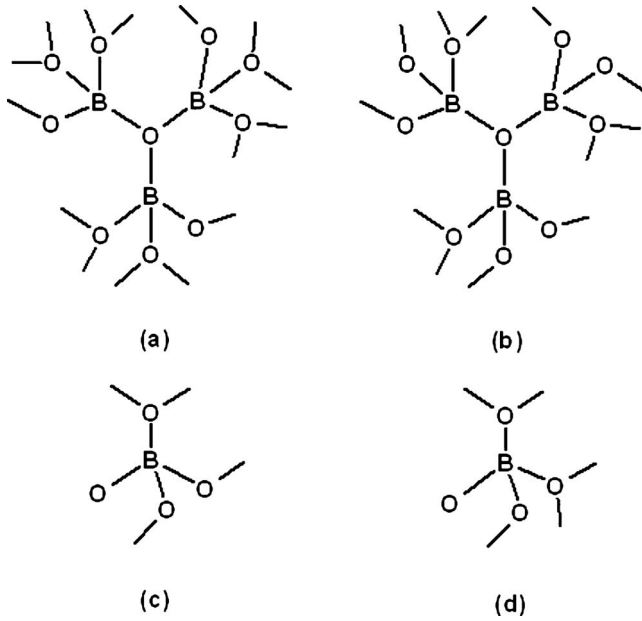


FIG. 10. Schematic presentation of tricluster arrangements for (a) the high-pressure form B_2O_3 II of crystalline boron oxide (Ref. 37) and (b) the $0.3Li_2O-0.7B_2O_3$ glass at the high-pressure side of zone III. Tricluster (b) coexists with borate tetrahedra [(c) and (d)] having nonbridging oxygen atoms for consistency with the results of molecular dynamics and the glass composition. Oxygen atoms are presented in schematics with one, two, or three bonds with boron to indicate oxygen in the nonbridging ($[^1]O$), twofold ($[^2]O$), and threefold ($[^3]O$) coordination, respectively.

The common characteristics of these crystals is that all borons are tetrahedrally coordinated in a three-dimensional network formed by $[^2]O$ and $[^3]O$ oxygen with the boron and oxygen atoms linked in complex ring structures. For example, the fundamental building block of $\beta-ZnB_4O_7$ involves eight BO_4 tetrahedra which form a six-membered ring linked to two three-membered rings. Each of these three-membered rings has two BO_4 tetrahedra in common with the six-membered ring. However, it is highly unlikely that such well-defined structures in crystals are present at high pressures in glass $0.3Li_2O-0.7B_2O_3$.

Returning to the tricluster of B_2O_3 II in Fig. 10(a) we note that it can be written as $[^{[4]}B_3 [^{[3]}O_3 [^{[2]}O_{3/2}]^0]$ which results in $O[B]=2.67$ and $[^2]O/[^3]O=0.5$. The characteristic tricluster for Li-borate glass should be negatively charged because of the presence of Li cations, and it should be consistent with the present MD results. Gradual modification of tricluster, Fig. 10(a), by increasing the number of $[^2]O$ atoms leads to the tricluster shown in Fig. 10(b) which satisfies exactly the MD result $[^2]O/[^3]O=1.5$. It is easily realized that tricluster, Fig. 10(b), correspond to $[^{[4]}B_3 [^{[3]}O_2 [^{[2]}O_3]^{-1}]$ and gives $O[B]=2.40$, which is very close to $O[B]=2.35$ found by MD. It is noted, however, that tricluster, Fig. 10(b), has no NBOs and its stoichiometry $[B_3O_5]^{-1}$ deviates from that of the average borate anion representing the simulated glass, i.e., $[B_{2.33}O_4]^{-1.01}$. In light of these facts we suggest that tricluster, Fig. 10(b), should coexists with borate tetrahedra having NBOs as well as $[^3]O$ and $[^2]O$ atoms. The latter units should be present at relatively small contents because of the

small fraction of NBOs found by simulation (approximately 4.3%). To allow for a variable number of $[^3]O$ and $[^2]O$ atoms in borate tetrahedra with NBOs we propose the units shown in Figs. 10(c) and 10(d) with stoichiometry

$$[^{[4]}B_1 [^{[3]}O_{1/3} [^{[2]}O_1 [^{[1]}O_1]^{-1.67}}$$

and

$$[^{[4]}B_1 [^{[3]}O_{2/3} [^{[2]}O_{1/2} [^{[1]}O_1]^{-1.34},$$

respectively. We consider now whether the coexistence of tricluster, Fig. 10(b), with borate tetrahedra, Figs. 10(c) and 10(d), is consistent with the present MD results.

Let us assume that the simulated ensemble of glass $0.3Li_2O-0.7B_2O_3$, which consists of 556 O atoms, 324 B atoms, and 140 Li ions, contains at high-pressures x triclusters, Fig. 10(b), y tetrahedra, Fig. 10(c), and z tetrahedra, Fig. 10(d). Then, it is straightforward to write the following equations:

$$\begin{aligned} [^2]O/[^3]O \text{ ratio} &= [3x + y + (1/2)z]/[2x + (1/3)y + (2/3)z] \\ &= 1.5, \end{aligned} \quad (1)$$

$$\text{B content,} \quad 3x + y + z = 324, \quad (2)$$

$$\text{Li content,} \quad x + 1.67y + 1.34z = 140, \quad (3)$$

$$\text{O content,} \quad 5x + 2.33y + 2.17z = 556. \quad (4)$$

Solving the system of Eqs. (1)–(3) gives $x=98.86$, $y=13.71$, and $z=13.71$; this solution satisfies also Eq. (4). Therefore, the high-pressure structure of glass $0.3Li_2O-0.7B_2O_3$ in zone III can be described in terms of interconnected BO_4 tetrahedra of which 91.5% participate in triclusters, Fig. 10(b), and 8.5% form tetrahedra, Figs. 10(c) and 10(d). It can be verified easily that this structural combination gives 4.9% NBOs and corresponds to an average oxygen coordination number of $O[B]=2.33$, both results being in good agreement with those found by simulation.

It would be of interest to know whether a tricluster of the type $[^{[4]}B_3 [^{[3]}O_2 [^{[2]}O_3]^{-1}]$, Fig. 10(b), could reflect a high-pressure and high-density ($\sim 3.5-3.8 \text{ g/cm}^3$) phase of Li-diborate crystal, where the densities in parentheses correspond to pressure values at the end of zone III. However, high-pressure Raman spectroscopy showed that this crystal transforms to an amorphous phase for pressures greater than 17 GPa.⁴⁰ In addition, the structure of this amorphous phase was found different from that of the normal Li-diborate glass.

The experimental findings of Refs. 2 and 3 showed similarities in the densification mechanisms of $v-B_2O_3$ and Li-diborate glass, both glasses exhibiting considerable differences when compared to the densification of Na-diborate glass. To search for the origin of these effects we intend to extend our calculations to borate glasses with differences in the NBO content and in the field strength of the modifying metal ion. Suitable glasses for such investigation are Li metaborate and Na diborate, respectively.

IV. CONCLUSIONS

In the present work we performed a detailed MD calculation concerning the effect of pressure on the structure of glass $0.3\text{Li}_2\text{O}-0.7\text{B}_2\text{O}_3$ at room temperature. We explored pressures spanning the wide range from 1 atm up to about 300 GPa and analyzed the evolution of both short- and the medium-range order structures in this glass system.

The structural transformations revealed by simulation were found in good agreement with the reported experimental results of Lee *et al.*² for pressures up to 30 GPa. We have distinguished three different structural zones as in the experiment with the addition of a fourth zone which is not accessible experimentally as it extends from ~ 80 to ~ 300 GPa. The first zone, which in the experiment extends from ambient to about 5 GPa, marks the onset of minor structural changes and appears quite narrow in our calculation. This originates probably from deficiencies of the employed potential model which produces more densely packed glasses.

The second zone extends from 5 to 15 GPa and corresponds to the rapid conversion of triangular to tetrahedral borate units ($^{[3]}\text{B} \rightarrow ^{[4]}\text{B}$), together with the coordination transformation of twofold to threefold oxygen ($^{[2]}\text{O} \rightarrow ^{[3]}\text{O}$). Zone III includes the wide range of pressures from 15 GPa to about 80 GPa and is characterized by a plateau where both boron and oxygen coordination numbers remain constant at

$\text{B}[\text{O}]=4$ and $\text{O}[\text{B}]\approx 2.35$. Simulations in zone III showed also that twofold and threefold oxygen atoms are present in the relative proportion $^{[2]}\text{O}/^{[3]}\text{O}=1.5$ and coexist with approximately 4.3% nonbridging oxygen atoms, NBOs. Besides the short-range structure, it was possible to determine medium-range order configurations in zone III with the overall structure being consistent with the glass composition and the simulation results. It was found in zone III that the borate network consists only of tetrahedral boron units with 91.5% of the $^{[4]}\text{B}$ boron atoms being engaged in tricluster arrangements of the type $^{[4]}\text{B}_3\text{O}_2\text{O}_3^{-1}$ [see Fig. 10(b)]. Besides this dominant structure, tetrahedral borate units with NBOs are also present and account for the remaining 8.5% of $^{[4]}\text{B}$ atoms [see Figs. 10(c) and 10(d)]. At the highest-pressure zone investigated here, zone IV from 80 to 300 GPa, it was found that fourfold boron atoms transform to fivefold and sixfold boron and threefold oxygen atoms to fourfold ones.

ACKNOWLEDGMENTS

Partial support of this work by the ‘‘Excellence in the Research Institutes’’ program, supervised by the General Secretariat for Research and Technology of Greece, is gratefully acknowledged.

*Corresponding author. FAX: 30-210 7273794; avegiri@eie.gr

- ¹R. J. Hemley, H. K. Mao, P. M. Bell, and B. O. Mysen, *Phys. Rev. Lett.* **57**, 747 (1986).
- ²S. K. Lee, P. J. Eng, H. K. Mao, Y. Meng, and J. Shu, *Phys. Rev. Lett.* **98**, 105502 (2007).
- ³S. K. Lee, P. J. Eng, H. K. Mao, and J. Shu, *Phys. Rev. B* **78**, 214203 (2008).
- ⁴J. S. Tse, D. D. Klug, and Y. Le Page, *Phys. Rev. B* **46**, 5933 (1992).
- ⁵W. Jin, R. K. Kalia, P. V. Vashishta, and J. P. Rino, *Phys. Rev. B* **50**, 118 (1994).
- ⁶R. G. Della Valle and E. Venuti, *Phys. Rev. B* **54**, 3809 (1996).
- ⁷M. M. Roberts, J. R. Wienhoff, K. Grant, and D. J. Lacks, *J. Non-Cryst. Solids* **281**, 205 (2001).
- ⁸A. Trave, P. Tangney, S. Scandolo, A. Pasquarello, and R. Car, *Phys. Rev. Lett.* **89**, 245504 (2002).
- ⁹K. Trachenko and M. T. Dove, *J. Phys.: Condens. Matter* **14**, 7449 (2002).
- ¹⁰L. Huang, L. Duffrène, and J. Kieffer, *J. Non-Cryst. Solids* **349**, 1 (2004).
- ¹¹Y. Liang, C. R. Miranda, and S. Scandolo, *Phys. Rev. B* **75**, 024205 (2007).
- ¹²A. M. Walker, L. A. Sullivan, K. Trachenko, R. P. Bruin, T. O. H. White, M. T. Dove, R. P. Tyer, I. T. Todorov, and S. A. Wells, *J. Phys.: Condens. Matter* **19**, 275210 (2007).
- ¹³S. K. Lee, K. Mibe, Y. Fei, G. D. Cody, and B. O. Mysen, *Phys. Rev. Lett.* **94**, 165507 (2005).
- ¹⁴A. C. Wright, C. E. Stone, R. N. Sinclair, N. Umesaki, N. Kitamura, K. Ura, N. Ohtori, and A. C. Hannon, *Phys. Chem. Glasses* **41**, 296 (2000).

- ¹⁵M. Grimsditch, A. Polian, and A. C. Wright, *Phys. Rev. B* **54**, 152 (1996).
- ¹⁶V. V. Brazhkin, Y. Katayama, K. Trachenko, O. B. Tsiok, A. G. Lyapin, E. Artacho, M. Dove, G. Ferlat, Y. Inamura, and H. Saitoh, *Phys. Rev. Lett.* **101**, 035702 (2008).
- ¹⁷J. Nicholas, S. Sinogeikin, J. Kieffer, and J. Bass, *Phys. Rev. Lett.* **92**, 215701 (2004).
- ¹⁸S. K. Lee, P. J. Eng, H. K. Mao, Y. Meng, M. Newville, M. Y. Hu, and J. F. Shu, *Nature Mater.* **4**, 851 (2005).
- ¹⁹K. Trachenko, V. V. Brazhkin, G. Ferlat, M. T. Dove, and E. Artacho, *Phys. Rev. B* **78**, 172102 (2008).
- ²⁰A. Takada, *Phys. Chem. Glasses* **45**, 156 (2004).
- ²¹L. Huang, M. Durandurdu, and J. Kieffer, *J. Phys. Chem. C* **111**, 13712 (2007); L. Huang, J. Nicholas, J. Kieffer, and J. Bass, *J. Phys.: Condens. Matter* **20**, 075107 (2008).
- ²²M. Guthrie, C. A. Tulk, C. J. Benmore, J. Xu, J. L. Yarger, D. D. Klug, J. S. Tse, H-k. Mao, and R. J. Hemley, *Phys. Rev. Lett.* **93**, 115502 (2004).
- ²³X. Hong, G. Shen, V. B. Prakapenka, M. Newville, M. L. Rivers, and S. R. Sutton, *Phys. Rev. B* **75**, 104201 (2007).
- ²⁴P. Richet, G. Hovis, and B. Poe, *Chem. Geol.* **213**, 41 (2004).
- ²⁵O. Ohtaka, A. Yoshiasa, H. Fukui, K. Murai, M. Okube, H. Takebe, Y. Katayama, and W. Utsumi, *J. Phys.: Condens. Matter* **14**, 10521 (2002).
- ²⁶J. P. Itie, A. Polian, G. Calas, J. Petiau, A. Fontaine, and H. Tolentino, *Phys. Rev. Lett.* **63**, 398 (1989).
- ²⁷T. Ishihara, Y. Shirakawa, T. Iida, N. Kitamura, M. Matsukawa, N. Ohtori, and N. Umesaki, *Jpn. J. Appl. Phys.* **38**, 3062 (1999).
- ²⁸G. Ferlat, T. Charpentier, A. P. Seitsonen, A. Takada, M. Lazzari, L. Cormier, G. Calas, and F. Mauri, *Phys. Rev. Lett.* **101**,

- 065504 (2008).
- ²⁹E. I. Kamitsos, A. P. Patsis, and G. D. Chryssikos, *J. Non-Cryst. Solids* **152**, 246 (1993); E. I. Kamitsos, *Phys. Chem. Glasses* **44**, 79 (2003).
- ³⁰Cristos-Platon E. Varsamis, A. Vegiri, and E. I. Kamitsos, *Phys. Rev. B* **65**, 104203 (2002).
- ³¹A. Vegiri, C. P. E. Varsamis, and E. I. Kamitsos, *Phys. Rev. B* **80**, 184202 (2009).
- ³²A. H. Verhoef and H. W. den Hartog, *J. Non-Cryst. Solids* **182**, 235 (1995).
- ³³W. Smith and T. Forester, *J. Mol. Graphics* **14**, 136 (1996).
- ³⁴M. Shibata, C. Sanchez, H. Patel, S. Feller, J. Stark, G. Sumcad, and J. Kasper, *J. Non-Cryst. Solids* **85**, 29 (1986).
- ³⁵C. K. Jayasankar, K. Ramanjaneya Setty, P. Babu, Th. Troster, and W. B. Holzapfel, *Phys. Rev. B* **69**, 214108 (2004).
- ³⁶M. Kodama, S. Feller, and M. Affatigato, *J. Therm Anal. Calorim.* **57**, 787 (1999).
- ³⁷C. T. Prewitt and R. D. Shannon, *Acta Crystallogr., Sect. B: Struct. Crystallogr. Cryst. Chem.* **24**, 869 (1968).
- ³⁸D. L. Corker and A. M. Glazer, *Acta Crystallogr., Sect. B: Struct. Sci.* **52**, 260 (1996).
- ³⁹H. Huppertz and G. Heymann, *Solid State Sci.* **5**, 281 (2003).
- ⁴⁰Y. Li and G. Lan, *J. Phys. Chem. Solids* **57**, 1887 (1996).